Atmospheric Research, 24 (1989) 273–284
Elsevier Science Publishers B.V., Amsterdam — Printed in The Netherlands

The Effects of the Nonsphericity and Size Distribution of Ice Crystals on the Radiative Properties of Cirrus Clouds

STEFAN KINNE and KUO-NAN LIOU

Space Science Division, NASA Ames Research Center, Moffett Field, CA 94035 (U.S.A.)
Department of Meteorology, University of Utah, Salt Lake City, UT 84112 (U.S.A.)

(Received January 23, 1989; accepted after revision May 23, 1989)

ABSTRACT

Kinne, S. and Liou, K.N., 1989. The effects of the nonsphericity and size distribution of ice crystals on the radiative properties of cirrus clouds. Atmos. Res., 24: 273–284.

Hexagonal ice crystals and equivalent ice spheres have significantly different single-scattering properties. Although the extinction cross-section for spheres with equivalent surface areas is about the same as that for nonspherical ice crystals randomly oriented in space, equivalent spheres produce more forward scattering and have smaller single-scattering albedos. On the basis of broad-band radiative transfer calculations, in this note we will illustrate that the assumption that ice particles are spheres with equivalent surface areas leads to an underestimate of the solar albedo of cirrus clouds. Furthermore, we show that, for a given optical thickness, small ice particles reflect more solar flux than large ice particles. This implies that the ice crystal size distribution could be extremely important in the determination of the solar albedo of cirrus clouds due to external radiative forcings in climatic perturbation experiments. In the thermal infrared region, absorption by ice crystals predominates and the effects of the nonsphericity and size distribution of ice crystals on infrared radiative transfer appear to be secondary.

RESUME

Des cristaux de glace hexagonaux et des sphères de glace équivalentes ont des propriétés de diffusion simple significativement différentes. Bien que la section efficace d'extinction pour des sphères soit à peu près la même que pour les cristaux non sphériques de surface équivalente orientés au hasard dans l'espace, les sphères produisent une diffusion arrière plus forte, et des albédos de diffusion simple plus faibles. Par des calculs de transfert radiatif à bande large, on montre dans cet article que l'hypothèse selon laquelle les particules de glace sont des sphères de surface équivalente conduit à une sous-estimation de l'albédo des cirrus. De plus, on montre que, pour une épaisseur optique donnée, les petites particules de glace réfléchissent plus de flux solaire que les grosses particules. Ce résultat signifie que la distribution dimensionnelle des cristaux de glace doit être extrêmement importante dans la détermination de l'albédo solaire des cirrus, à cause des forçages radiatifs externes dans les expériences de perturbation climatique. Dans la région infrarouge thermique, l'absorption par les cristaux de glace prédomine, et les effets de la non sphéricité et de la distribution dimensionnelle des cristaux de glace sur le transfert radiatif infrarouge apparaissent secondaires.

0169-8095/89/$03.50

INTRODUCTION

Cirrus clouds have been identified as presenting one of the major unresolved problems in weather and climate research (Liou, 1986). From aircraft observations, it has been determined that cirrus clouds are largely composed of nonspherical bullets, columns, and plates (Heymsfield, 1975). There are also significant variations in the size distribution of these ice crystals. In order to determine the radiative properties of cirrus clouds, information on the scattering and absorption of nonspherical ice crystals is necessary. Based on a ray tracing technique, Takano and Liou (1989a) developed a light scattering and absorption program for hexagonal ice crystals. They showed that there are significant differences in the single-scattering albedo and asymmetry factor between hexagonal ice crystals and spheres with equivalent volumes or surface areas. Moreover, substantial differences are also evident between spherical and nonspherical ice crystals in terms of their reflected and transmitted intensities, and planetary albedo (Takano and Liou, 1989b). However, the preceding results were derived only for visible wavelengths.

In this note, we wish to investigate the effects of the nonsphericity and size distribution of ice crystals on the broadband radiative properties of cirrus clouds, and to assess their potential climatic impact. We begin with a discussion of the single-scattering properties of hexagonal ice crystals and spheres with equivalent surface areas. The effects of the nonsphericity and size distribution of ice crystals on cirrus radiative properties are then presented. Finally, we discuss the significance of the microphysical composition of cirrus clouds in climatic processes, based on an examination of the net fluxes at the top of the atmosphere (TOA).

SINGLE-SCATTERING CALCULATIONS FOR ICE PARTICLES

Single-scattering calculations involving the observed ice crystal size distribution in cirrus clouds were carried out using the scattering and absorption program for hexagonal ice crystals developed by Takano and Liou (1989a) and the Mie scattering program for spherical particles. There have been a number of published reports on aircraft observations of the ice crystal size distribution. Heymsfield (1975) presented ice crystal size distributions for cirrostratus (Cs) and cirrus uncinus (Ci). The latter has a bimodal distribution with a second maximum concentration peak at about 500 μm. Heymsfield and Platt (1984) classified the ice crystal size distribution according to warm ($-30°C$) and cold ($-55°C$) cirrus clouds. Griffith et al. (1980) carried out aircraft observations of the thermal infrared radiative properties and microphysics of tropical cirrus clouds. The observed ice crystal size distributions reported by these authors are given in Fig. 1.

For scattering and radiative transfer calculations, we have selected the ice

crystal size distributions for Cs and Ci that were presented by Heymsfield (1975). These size distributions appear to cover the various observed values for ice crystals shown in Fig. 1. We have discretized the ice crystal size distributions in five regions where the aspect ratios ($L/2a$) used are 20/20, 50/40, 120/60, 300/100, and 75/160 μm/μm, with L the length and $2a$ the diameter. These aspect ratios approximately correspond to the observations reported by Ono (1969) and Auer and Veal (1970). For single-scattering calculations, the refractive indices for ice compiled by Warren (1984) were used.

To investigate the effects of the nonsphericity of ice crystals on the radiative properties of cirrus clouds, we have also performed calculations for the single-scattering properties of ice particles by assuming that they are spherical and using the Mie scattering program. However, spheres with either equivalent volumes or equivalent surface areas may be used. Spheres with equivalent surface areas provide the same geometrical cross-section as that for randomly oriented nonspherical particles and, hence, will give approximately the same extinction cross-section. The optical thickness will be about the same if the number density of ice crystals and geometric thickness of the cloud remain the same for spherical and nonspherical particles. For this reason, we have used spheres with equivalent surface areas in the comparison study.

The effects of the nonsphericity of ice crystals are most pronounced in the solar radiative properties of cirrus clouds. In the thermal infrared region, the

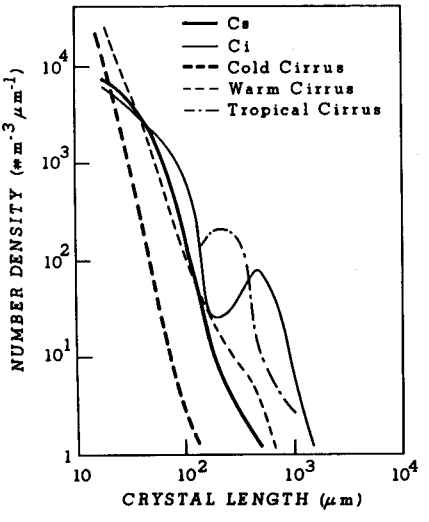

Fig. 1. The observed ice crystal size distributions for cirrus clouds as functions of the crystal length. Th heavy and thin solid lines denote the size distributions for cirrostratus (*Cs*) and cirrus uncinus (*Ci*), respectively, presented by Heymsfield (1975). The heavy and thin dashed lines represent the size distributions for warm (−30°C) and cold (−55°C) cirrus clouds, respectively, classified by Heymsfield and Platt (1984). The dashed and dotted line is the size distribution reported by Griffith et al. (1980) for tropical cirrus clouds.

TABLE I

Comparison of the co-single-scattering albedos, $1-\omega$, between hexagonal ice crystals and surface-area equivalent spheres for a number of wavelengths and particle sizes

$\lambda(\mu m)$	20/20*[1]	11.7*[2]	50/40	25.4	120/60	45.7	300/100	90.5	750/160	177
.55	.622-6	.766-6	.154-5	.164-5	.265-5	.274-5	.453-5	.577-5	.758-5	.107-4
1.0	.243-3	.270-3	.518-3	.574-3	.860-3	.965-3	.152-2	.188-2	.254-2	.355-2
1.6	.161-1	.191-1	.337-1	.386-1	.536-1	.599-1	.880-1	.110	.130	.190
2.2	.409-1	.455-1	.818-1	.916-1	.125	.145	.187	.239	.250	.353
3.0	.466	.503	.469	.485	.469	.477	.469	.472	.469	.470
10.0	.309	.309	.421	.461	.450	.497	.470	.493	.476	.485

*[1]Hexagonal ice crystals with dimensions, $L/2a$, where L is the length (μm) and $2a$ is the diameter (μm).
*[2]Spheres of equivalent surface areas with radius r (μm).

TABLE II

Comparison of the asymmetry factor, g, between hexagonal ice crystals and surface-area equivalent spheres for a number of wavelengths and particle sizes

$\lambda(\mu m)$	20/20	11.7	50/40	25.4	120/60	45.7	300/100	90.5	750/160	177
.55	.770	.868	.778	.884	.816	.888	.843	.888	.859	.890
1.0	.776	.853	.785	.882	.822	.887	.849	.891	.865	.891
1.6	.790	.841	.805	.876	.846	.898	.880	.911	.904	.924
2.2	.819	.896	.842	.899	.883	.916	.917	.937	.938	.956
3.0	.957	.970	.986	.974	.972	.975	.974	.976	.975	.976
10.0	.886	.938	.941	.948	.962	.976	.974	.983	.979	.984

effect of nonsphericity is probably secondary, due to large absorption of ice. We have undertaken single-scattering and absorption calculations for a number of wavelengths in the solar spectrum. The calculations at 0.55 μm cover not only the visible region, but also the UV part of the solar spectrum. This is due to the fact that the refractive indices of ice are almost constant in these wavelength regions. However, in the near IR part of the solar spectrum, the imaginary refractive indices are highly wavelength-dependent. After numerical experimentations, we find that the division of the near IR spectrum in four bands centered at 1.0, 1.6, 2.2 and 3.0 μm is sufficient to accurately derive the broadband solar radiative properties, 2.2, and 3.0 μm, corresponding to the center wavelengths in the solar bands, which were divided for radiative transfer calculations covering the visible and near infrared spectrum. The wavelengths were selected in connection with gaseous absorption due to water vapor in the visible and near infrared regions. In the ultraviolet region, the single-scattering parameters for ice crystals are assumed to be the same as those for

the visible band since the index refraction for ice does not vary significantly over these bands. We have used a wavelength of 10 μm for calculations of the single-scattering parameters for ice particles in the thermal infrared region. We recognize that, at this wavelength, the geometric ray tracing technique may not be accurate for small hexagonal crystals (e.g. 20/10 μm). This is an area that requires improved calculations.

Listed in Table I are the co-single-scattering albedos, $1-\omega$, for a number of wavelengths and particle size for hexagonal ice crystals and spheres with equivalent surface areas. The single-scattering albedo is defined by:

$$\omega = \sigma_s / \sigma_e$$

where σ_s and σ_e denote the scattering and extinction cross-sections, respectively. The co-single-scattering albedos for hexagonal ice crystals are smaller than those for spheres. This implies that spheres with equivalent geometric cross-sections will absorb more solar flux than nonspherical particles. In particular, there are significant differences between large ice particles in the near infrared wavelengths of 1.0, 1.6, and 2.2 μm. In Table II we present the results for the asymmetry factor, g, which is defined by:

$$g = \frac{1}{2} \int_{-1}^{1} P(\theta) \cos\theta \, \mathrm{dcos}\, \theta,$$

where P is the phase function and θ the scattering angle. Spheres have larger asymmetry factors than hexagonal ice crystals. Thus there would be more forward scattering in the case of spheres. This is particularly evident for small ice crystals illuminated by visible and near infrared radiation. Absorption is small in the visible wavelength. Thus the differences in the visible radiative properties between hexagonal ice crystals and ice spheres are primarily caused by scattering.

THE RADIATIVE PROPERTIES OF CIRRUS CLOUDS

In order to obtain the broadband radiative properties of cirrus clouds, radiative transfer calculations were carried out for the entire solar and thermal infrared spectral regions. We have divided the solar and thermal infrared regions into various spectral bands, according to the location of absorbing gases. All the data for gaseous absorption were based on spectral transmittances computed from line-by-line data. A set of equivalent absorption coefficients and weights for each spectral band was derived from an exponential fitting program. For applications to inhomogeneous atmospheres, the scaling approximation was used. Details concerning the determination of equivalent absorption coefficients for incorporation in the radiative transfer program can be found in Kinne (1987).

The radiative transfer program used in the present study follows the matrix-

operator method, which is based on the adding principle for radiative transfer. This principle uses a ray tracing technique (see, e.g., Takano and Liou, 1989b) and allows the optical properties for a combination of layers, in terms of those for each individual layer, to be expressed. The zenith-angle-dependence is incorporated through a discretization of the direction, which is obtained by dividing the range of the cosine of the solar zenith angle. The application of the adding principle to an inhomogeneous atmosphere is carried out by dividing the atmosphere into a number of homogenous layers. The resulting intensities for various directions at each layer boundary are summed to obtain the hemispheric fluxes (Kinne, 1987). The solar constant and surface albedo used are 1360 W m^{-2} and 0.15, respectively. Cirrus clouds are inserted in the standard atmosphere between 9 and 11 km in the radiative transfer calculations.

Fig. 2 shows the increase in the planetary albedo, as a function of the solar zenith angle, due to the presence of two types of cirrus clouds (with respect to the planetary albedo of the clear atmosphere). Here, the planetary albedo is defined as the ratio of the reflected solar flux to the incoming solar flux at the TOA. For Cs, optical thicknesses of 0.1, 1, and 3 were used in the calculations. For Ci, optical thicknesses of 1, 3, and 10 were used. These values represent realistic optical thicknesses for cirrus clouds. For both cloud types, the increase in the planetary albedo is smaller in the case with equivalent spheres. This is primarily due to the fact that equivalent spheres have stronger forward scat-

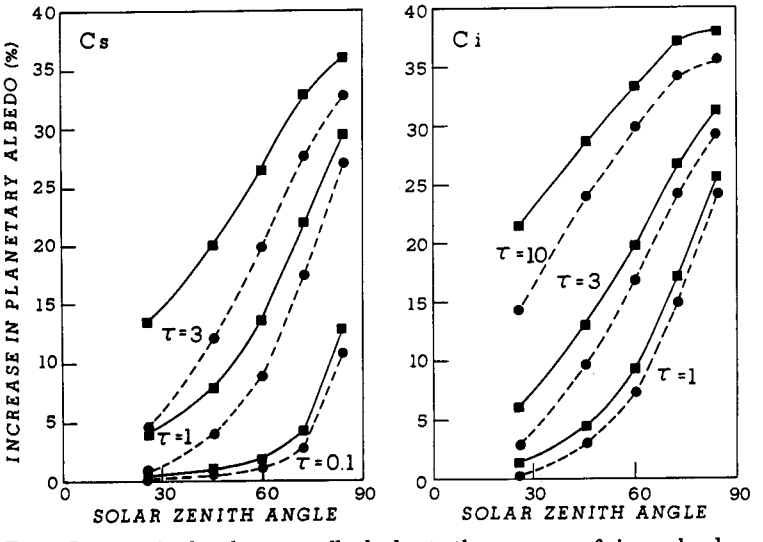

Fig. 2. Increase in the planetary albedo due to the presence of cirrus clouds composed of hexagonal ice crystals (black square) and ice spheres with equivalent surface areas (black circles) as a function of the solar zenith angle for two types of cirrus clouds. For Cs, the optical thicknesses used in the calculations are 0.1, 1, and 3, while for Ci, they are 1, 3, and 10. These diagrams illustrate the significance of the nonsphericity of ice crystals in planetary albedo values.

tering and thereby reduce the reflected solar fluxes. The reduction in the planetary albedo depends on the effective optical depth, which is a function of the optical depth and solar zenith angle, as well as the cloud type. For Cs with an optical thickness of 1, the assumption of sphericity for ice crystals leads to an underestimate of the planetary albedo by about 5% or more. The effects of nonsphericity on the planetary albedo are less significant in the case of Ci. For example, for an optical thickness of 1, the spherical assumption underestimates the planetary albedo by only about 2%. It is noted that an increase of a few percent in the planetary albedo would offset the surface temperature increase due to a doubling of CO_2. This suggests that the ice crystal size distribution could play a major role in climatic perturbations due to external radiative forcing.

In order to illustrate the importance of the ice crystal size distribution in the planetary albedo, we replotted the increase in the planetary albedo as a function of cloud type for a given optical thickness, as shown in Fig. 3. Clouds containing small ice crystals would have larger albedos. In the case of Cs vs Ci, differences of about 4% are seen for an optical thickness of 1. For an optical thickness of 3, a difference of as much as 10% is observed. As described in the preceding section, small ice particles have larger geometric areas than large ice particles. For this reason, Cs reflects more solar flux than Ci for a given optical thickness. The general effects of the particle size distribution on the planetary

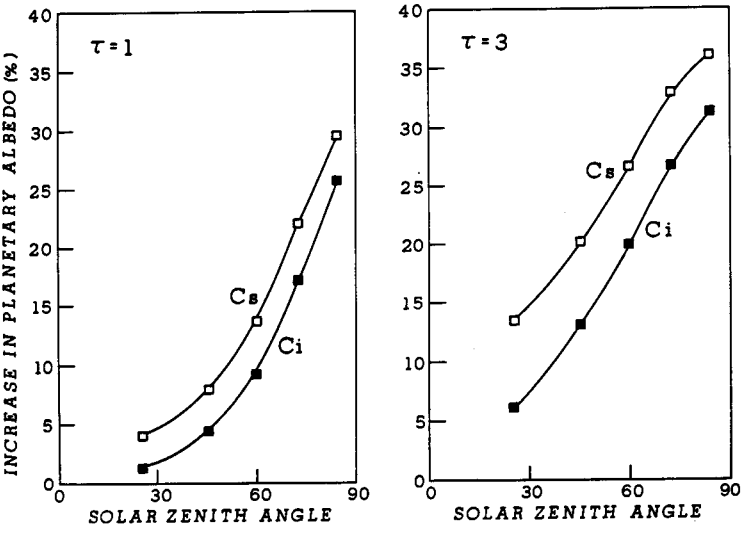

Fig. 3. Increase in the planetary albedo due to the presence of Cs (square) and Ci (black square) composed of hexagonal ice crystals as a function of the solar zenith angle. Two optical thicknesses of 1 and 3 are shown. These diagrams illustrate the importance of the ice crystal size distribution in planetary albedo values.

albedo are universal, regardless of the particle shape. Thus these effects can be applied to clouds composed of spherical droplets.

It is appropriate to investigate the effects of the nonsphericity and size distribution on the transfer of thermal infrared radiation in terms of the effective downward emissivity, defined by:

$$\epsilon(Z_b) = \frac{F^{\downarrow}(Z_t) - F^{\downarrow}(Z_b)}{F^{\downarrow}(Z_t) - \sigma T_b^4}$$

where Z_t and Z_b are cloud top and base heights, respectively, σ the Stefan-Boltzmann constant, and T_b the cloud base temperature. Because ice absorbs significantly over the entire infrared region, the shape of ice crystals has little effect on the downward emissivity. For a given cloud type consisting of hexagonal ice crystals or spheres with equivalent surface areas, differences in the downward emissivity are less than 1% for optical depths (at 0.55 μm) of 0.1 to 3 (Cs), and 1 to 10 (Ci). With respect to the ice crystal size distribution, the downward emissivity as a function of the optical thickness for Cs and Ci is presented in Fig. 4. For optical thicknesses of 1 to 3, where overlap occurs, the differences are less than about 1%. Thus, whether the cloud contains small or large ice crystals is not critical to the cloud emissivity value. The emissivity varies from about 0.5 to 0.8 for optical depths of from 1 to 3. The emissivity value can be as small as 0.2 for an optical depth of 0.1 in the case of Cs. How-

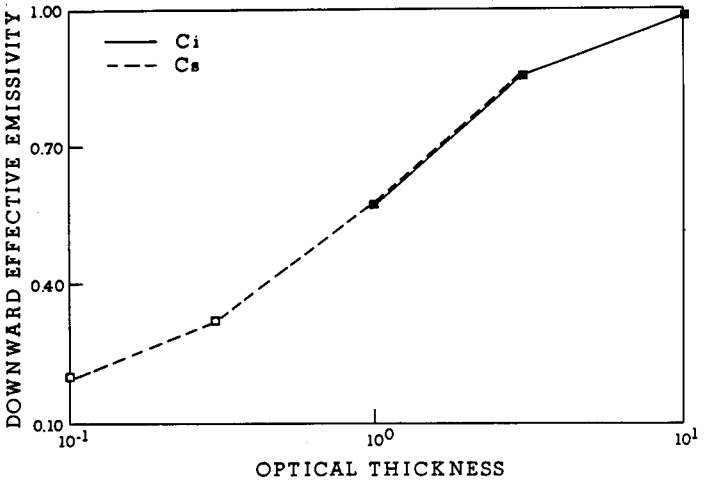

Fig. 4. Downward effective emissivity as a function of the optical thickness (at 0.55 μm). For Cs, the optical thicknesses used in the broadband infrared calculation are 0.1, 0.3, 1, and 3 (dashed line), while for Ci, they are 1, 3, and 10. There are overlaps in the optical thickness range of from 1 to 3. The dotted line near the bottom represents the downward emissivity for an atmosphere without clouds. In this case, the downward emissivity is solely contributed from absorbing gases.

ever, it reaches a blackbody value of 1 for an optical depth of 10 in the case of Ci.

In summary, the nonsphericity and size distribution of ice crystals would have a significant effect on the transfer of solar fluxes in cirrus clouds. The solar albedo effects are significantly modulated by the cloud composition, in terms of the shape of ice particles and their size distribution. On the other hand, the effects of the nonsphericity and size distribution of ice crystals on the transfer of thermal infrared fluxes would be insignificant because of the large absorption of ice. Thus the greenhouse effects of cirrus clouds depend primarily on the optical thickness of the clouds and less on the shape factor and size distribution of ice crystals.

CLIMATIC ASSESSMENT AND CONCLUSIONS

In order to assess the potential effects of the nonsphericity and size distribution of ice crystals on the radiation budget of the earth and the atmosphere, we computed the net flux changes ($W\ m^{-2}$) for both solar and thermal infrared radiation at the TOA due to the presence of cirrus clouds. An increase (decrease) in the net flux at the TOA would imply a warming (cooling) of the earth–atmosphere system.

In the presentation, we use optical thicknesses of 0.1 and 1 for Cs, and 1 and 10 for Ci. Fig. 5 illustrates the net flux change as a function of the solar zenith angle. As reported in the preceding section, the assumption regarding the shape of ice crystals does not significantly alter the infrared emission. However, the use of surface equivalent spheres leads to a reduction in the planetary albedo as a result of stronger forward scattering with respect to hexagonal ice crystals, as demonstrated in Figs. 2 and 3. By combining the solar albedo and infrared emission effects, the net flux at the TOA may be increased or decreased depending on the cloud optical depth and solar zenith angle. The position of the sun determines the amount of solar flux available to the earth–atmosphere system. In the case of Cs with an optical depth of 0.1, warming takes place in the case with hexagonal ice crystals when the solar zenith angle is less than about 60°. The use of surface equivalent ice spheres in the calculation increases the net flux at the TOA by about 5 $W\ m^{-2}$. For Ci with an optical depth of 10, cooling occurs when the solar zenith angle is less than about 70°. This cooling would be significantly increased if surface equivalent ice spheres were replaced by hexagonal ice crystals in the radiation budget analysis. For an optical depth of 1, warming is evident for most solar zenith angles. The assumption of surface equivalent spheres leads to a significant overestimate of the warming. For Cs, the overestimate could be as large as 40 $W\ m^{-2}$. In the case of Ci with an optical thickness of 10, warming occurs for very low solar angles due to the small solar fluxes available to the earth–atmosphere system. As a result, the thermal infrared greenhouse effects outweigh the solar albedo

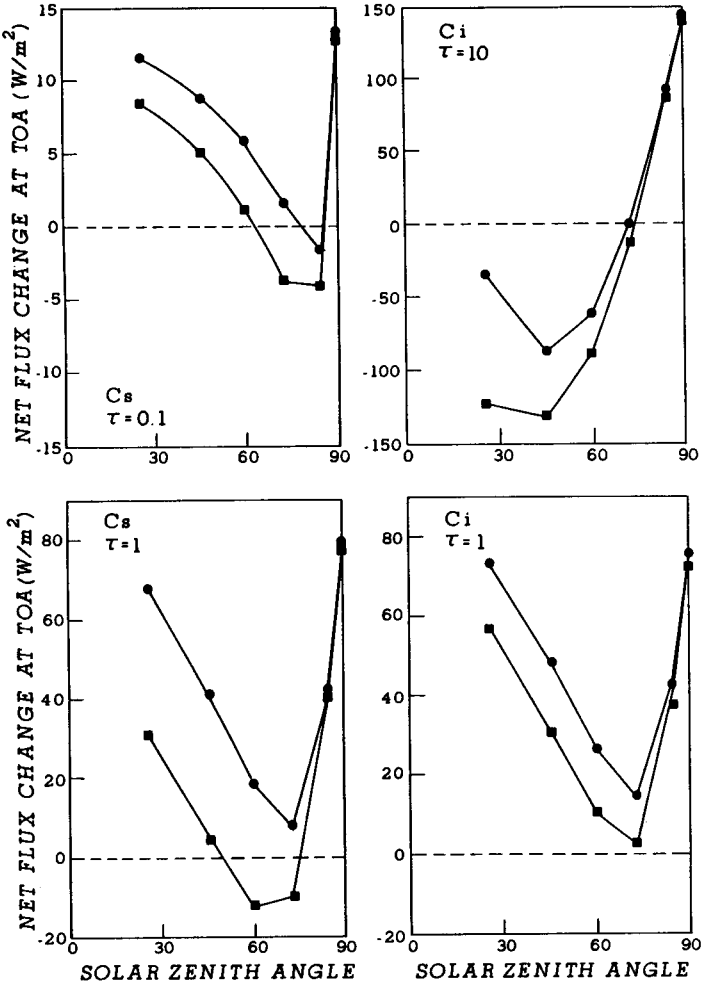

Fig. 5. The change in net fluxes at the TOA due to the presence of cirrus clouds as a function of the solar zenith angle. Positive and negative values represent warming and cooling of the earth-atmosphere system, respectively. The effects of the nonsphericity of ice crystals on the net fluxes at the TOA are shown for optical thicknesses of 0.1 and 1 in the case of Cs and for optical thicknesses of 1 and 10 in the case of Ci. Curves with black squares and black circles denote the results using hexagonal ice crystals and spheres with equivalent surface areas in the radiation budget analysis, respectively. The effects of the ice crystal size distribution (Cs versus Ci) on the net fluxes at the TOA can be seen in the lower diagrams with an optical thickness of 1.

effects. When the solar zenith angle is equal to 90°, at night, the presence of cirrus clouds produces significant increases in net fluxes at the TOA. In this case, clouds function as greenhouse elements.

As pointed out previously, the approximation of spheres with equivalent surface areas will give about the same optical thickness as randomly oriented ice

crystals. For this reason, this approximation was used in the preceding analysis of the effects of nonsphericity on the radiation budget. Spheres with equivalent volumes may also be used to approximate the radiative properties of nonspherical ice crystals. Volume equivalent spheres will produce about the same mass as randomly oriented ice crystals. However, this approximation will give a smaller extinction cross-section, and hence, a smaller optical thickness. It is quite clear that neither surface nor volume equivalent spheres can adequately approximate nonspherical ice crystals in terms of their radiative properties.

With respect to the effects of the ice crystal size distribution, we examine the graphs corresponding to an optical thickness of 1. Cs, which contains small ice crystals, reflects more solar flux than Ci, as pointed out in the preceding section. Thus the net flux increases at the TOA are larger for clouds composed of large ice crystals, regardless of the shape factor. The greenhouse effects predominate when Ci has an optical thickness of less than about 3. However, for Cs, optical thicknesses smaller than 1 would produce greenhouse warming. It is clear that the ice crystal size distribution is critically important in the determination of the prevalence of greenhouse-versus-albedo effects. The solar zenith angles in the tropics are normally smaller than those in middle and high latitudes. For this reason, the warming produced by thin cirrus in the tropics would be much more pronounced than in other latitudes.

In this note, we have demonstrated that the composition of cirrus clouds, in terms of the shape and size distribution of ice crystals, plays an important role in the determination of the radiative properties of clouds. These factors must be accounted for in the discussion of the climatic effects of cirrus clouds over the globe.

ACKNOWLEDGEMENTS

This research was supported, in part, by NASA Grants NAG5-732 and NAG5-1050. We thank Y. Takano for providing the single-scattering parameters for use in the present calculations. S. Kinne was supported by the NRC through NASA's Climate Program, managed by R. Schiffer.

REFERENCES

Auer, A.H., Jr. and Veal, D.L., 1970. The dimension of ice crystals in natural clouds. J. Atmos. Sci., 27: 919–926.

Griffith, K.T., Cox, S.K. and Knollenberg, R.G., 1980. Infrared radiative properties of tropical cirrus clouds inferred from aircraft measurements. J. Atmos. Sci., 37: 1077–1087.

Heymsfield, A.J., 1975. Cirrus uncinus generating cells and the evolution of cirroform clouds. J. Atmos. Sci., 32: 799–805.

Heymsfield, A.J. and Platt, C.M.R., 1984. A parameterization of the particle size spectrum of ice

clouds in terms of the ambient temperature and the ice water content. J. Atmos. Sci., 41: 846-855.

Kinne, S., 1987. Parametrization of Radiative Transfer in the Earth's Atmosphere with Specific Applications to Clouds. Ph.D. dissertation, University of Utah, Salt Lake City, 108 pp.

Liou, K.N., 1986. Influence of cirrus clouds on weather and climate processes: a global perspective. Mon. Weather Rev., 114: 1167-1199.

Ono, A., 1969. The shape and riming properties of ice crystals in natural clouds. J. Atmos. Sci., 26: 138-147.

Takano, Y. and Liou, K.N., 1989a. Radiative transfer in cirrus clouds, I. Single scattering and optical properties of hexagonal ice crystals. J. Atmos. Sci., 46: 3-20.

Takano, Y. and Liou, K.N., 1989b. Radiative transfer in cirrus clouds, II. Theory and computation of multiple scattering in an anisotropic medium. J. Atmos. Sci., 46: 21-38.

Warren, S.G., 1984. Optical constants of ice from the ultraviolet to the microwave. Appl. Opt., 23: 1206-1225.